Sim1 is Required for the Migration and Axonal Projections of V3 Interneurons in the Developing Mouse Spinal Cord

Jake Blacklaws,[1] Dylan Deska-Gauthier,[1] Christopher T Jones,[2] Yanina L. Petracca,[3] Mingwei Liu,[1] Han Zhang,[1] James P. Fawcett,[4] Joel C. Glover,[5] Guillermo M. Lanuza,[3] Ying Zhang[1]

[1] Department of Medical Neuroscience, Dalhousie University, Halifax, Nova Scotia, Canada B3H 4R2

[2] Department of Mathematics & Statistics, Dalhousie University, Halifax, Nova Scotia, Canada B3H 4R2

[3] Developmental Neurobiology Lab, Instituto Leloir and Consejo Nacional de Investigaciones Científicas y Técnicas (IIBBA-CONICET). Av Patricias Argentinas 435, Buenos Aires 1405, Argentina

[4] Departments of Pharmacology and Surgery, Dalhousie University, Halifax, Nova Scotia, Canada B3H 4R2

[5] Department of Physiology, Institute of Basic Medical Sciences, Faculty of Medicine, University of Oslo, Oslo, Norway

Received 3 November 2014; revised 15 January 2015; accepted 16 January 2015

ABSTRACT: **V3 spinal interneurons (INs) are a group of excitatory INs that play a crucial role in producing balanced and stable gaits in vertebrate animals. In the developing mouse spinal cord, V3 INs arise from the most ventral progenitor domain and form anatomically distinctive subpopulations in adult spinal cords. They are marked by the expression of transcription factor Sim1 postmitotically, but the function of Sim1 in V3 development remains unknown. Here, we used *Sim1^{Cre};tdTomato* mice to trace the fate of V3 INs in a Sim1 mutant versus control genetic background during development. In *Sim1* mutants, V3 INs are produced normally and maintain a similar position and organization as in wild types before E12.5. Further temporal analysis revealed that the V3 INs in the mutants failed to migrate properly to form V3 subgroups along the dorsoventral axis of the spinal cord. At birth, in the *Sim1* mutant the number of V3 INs in the ventral subgroup was normal, but they were significantly reduced in the dorsal subgroup with a concomitant increase in the intermediate subgroup. Retrograde labeling at lumbar level revealed that loss of Sim1 led to a reduction in extension of contralateral axon projections both at E14.5 and P0 without affecting ipsilateral axon projections. These results demonstrate that *Sim1* is essential for proper migration and the guidance of commissural axons of the spinal V3 INs.** Develop Neurobiol 00: 000–000, 2015

Keywords: **spinal cord; Sim1 transcription factor; V3 Interneurons; cell migration; axon guidance**

Correspondence to: Y. Zhang (ying.zhang@dal.ca).

Contract grant sponsor: Natural Sciences and Engineering Research Council of Canada; contract grant numbers: 38620 (to Y.Z.) and 341898 (to J.P.F).

Contract grant sponsor: Argentine Agency of Science; contract grant number: PICT2011-1350 (to G.M.L).

Contract grant sponsor: Norwegian Research Council and University of Oslo (to J.C.G.).

The authors declare no competing financial interests.

J.B. and D.D.-G. contributed equally to this work.

Additional Supporting Information may be found in the online version of this article.

Published online 00 Month 2015 in Wiley Online Library (wileyonlinelibrary.com).
DOI 10.1002/dneu.22266

INTRODUCTION

Interneurons (INs) in the spinal cord mediate and process descending inputs from the brain as well as inputs from sensory afferents, and thus, play crucial roles in the control and regulation of motor activity (Pearson, 1993; Grillner et al., 2005; Rossignol et al., 2006). INs also comprise the local circuitry, including the locomotor Central Pattern Generator, which generates the basic rhythm and patterning of motor outputs (Kiehn and Kullander, 2004; Goulding, 2009).

Studies in the developing vertebrate neural tube have identified 11 progenitor domains in the spinal cord that give rise to motor neurons (MNs) as well as six dorsal (dI1–6) and four ventral (V0–3) cardinal IN populations (Jessell, 2000; Goulding and Pfaff, 2005). Some of these IN populations, particularly those that settle in the ventral spinal cord, play distinct roles in controlling different aspects of locomotion (Lanuza et al., 2004; Gosgnach et al., 2006; Crone et al., 2008; Zhang et al., 2008, 2014; Zagoraiou et al., 2009; Talpalar et al., 2013).

Embryonically, IN classes are defined by the expression of specific transcription factors, some of which function in developmental processes underlying IN integration necessary for locomotor circuit formation. For example, Evx-1 plays a major role in both the ventromedial migratory pathway and commissural axonal projection patterns of V0 INs (Moran-Rivard et al., 2001; Pierani et al., 2001). Likewise, in mice lacking En-1, axons from the V1 INs fasciculate irregularly and exhibit decreased synaptic connectivity with MNs (Saueressig et al., 1999).

V3 INs are a group of excitatory spinal INs that arise from the Nkx2.2-expressing ventral-most progenitor domain (p3) (Briscoe et al., 1999; Goulding et al., 2002; Zhang et al., 2008, Carcagno et al., 2014). These neurons selectively express the transcription factor single-minded 1 (Sim1) on becoming postmitotic. In the mature mouse spinal cord Sim1 positive V3 INs assemble into anatomically and electrophysiologically distinct subgroups in the lower thoracic and upper lumbar regions (Borowska et al., 2013). Blocking synaptic transmission in V3 INs leads to defects in gait, suggesting an important role of V3 INs in establishing normal locomotion (Zhang et al., 2008).

Sim1 is a member of the basic helix-loop-helix/Per-Arnt-Sim (bHLH/PAS) family of transcription factors initially described in *Drosophila* (Kewley et al., 2004). Mouse *Sim1* is expressed in several regions of the central nervous system (CNS) during development and has been shown to play a crucial role in axon guidance (Marion et al., 2005; Schweitzer et al., 2013) and neuronal migration (Michaud et al., 1998; Xu and Fan, 2007) in the brain. To date, however, the role(s) of Sim1 in the development and differentiation of spinal V3 INs has not been investigated.

Here, we have followed the anatomical development of spinal V3 INs by genetic labeling in a control (*Sim1*$^{cre/+}$*;tdTomato*) versus a Sim1 mutant (*Sim1*$^{cre/lacZ}$*;tdTomato*) genetic background during the embryonic and perinatal period. We demonstrate that Sim1 is crucial for the proper migration and spatial distribution of V3 INs, and for the proper formation of V3 axonal trajectories, revealing a novel role for this transcription factor in the development of the spinal cord.

MATERIALS AND METHODS

Mouse Strains

Sim1$^{Cre/+}$, *Sim1*$^{tauLacZ/+}$, and *tdTomato* Ai14 conditional reporter (referred as *tdTom*) mice were generated and genotyped as previously described (Michaud et al., 1998; Marion et al., 2005; Zhang et al., 2008; Madisen et al., 2010). *Sim1*$^{Cre/+}$*;tdTom;* and *Sim1*$^{tauLacZ/+}$ were crossed to generate *Sim1*$^{Cre/tauLacZ}$*;tdTom*, which allows fate mapping of V3 INs in *Sim1* knockout mice. *Sim1*$^{Cre/+}$*;tdTom* animals served as controls. All procedures were performed in accordance with the Canadian Council on Animal Care and approved by the University Committee on Laboratory Animals at Dalhousie University.

Spinal Cord Tissue Processing

Fertilization was identified by the presence of a vaginal plug. The morning of discovery was defined as embryonic day 0.5 (E0.5). Embryonic spinal cords were obtained at E11.5, E12.5, and E14.5. Prior to surgery, pregnant mice were anaesthetized by intraperitoneal injection of a mixture of ketamine (60 mg/kg) and xylazine (12 mg/kg) and euthanized by cervical dislocation. Mouse embryos were then collected by cesarean section and placed in Ringer's Solution (6.49 g/L NaCl; 0.23 g/L KCl; 1.98 g/L D-Glucose; 2.1 g/L NaHCO3; 0.31 g/L MgSO4; 0.37 g/L CaCl2; 0.15 g/L KH2PO4) bubbled with 95% O_2/5% CO_2 with a maintained pH of 7.4. Postnatal day (P) 0 mice were euthanized via decapitation followed by spinal cord removal.

In Situ Hybridization

Nonradioactive *in situ* hybridization was performed essentially as previously described (Carcagno et al., 2014). Briefly, sections were fixed 15 min with paraformaldehyde (PFA) 4% in PBS and washed with PBS-DEPC. Tissue was treated with proteinase K (3 μg/mL, 3 min), followed by

PFA 4% for 10 min and PBS washes. Slides were incubated in triethanolamine-acetic anhydrate pH 8.0 for 10 min, permeabilized with Triton X-100 1% in PBS for 30 min, and washed with PBS. Sections were incubated for 2 h with hybridization solution (50% formamide, 5× SSC, 5× Denhardt solution, 250 μg/mL yeast tRNA). Digoxigenin-labeled RNA probes were generated by *in vitro* transcription using T7 RNA polymerase (Promega), digoxigenin-UTP (Roche), rNTPs (Promega), and polymerase chain reaction (PCR)-amplified products or linearized plasmids as templates. RNA probes used were mSim1 (Zhang et al., 2008), mNkx2.2 (Briscoe et al., 1999), mUncx (Mansouri et al., 2000), and mvGluT2 (Slc17a6) (Lanuza et al., 2004).

Retrograde Axonal Tracing with Biotin-Conjugated Dextran Amine

Isolated spinal cords were subjected to retrograde axonal tracing with biotin-conjugated dextran amine (BDA) using a previously described method (Supporting Information Fig. S1; Glover, 1995; Nissen et al., 2005). Briefly, 3 kDa BDA was dissolved in a small drop (1 μL) of water. Small quantities were collected on the tip of a needle (BD PrecisionGlide, 0.45 × 10 mm^2) to form a small crystal. Lumbar (L) segments were identified by their respective ventral roots, L1–L6. In E12.5 embryos, the most accurate landmark for the start of the lumbar region was the bottom of the rib cage and associated vertebrae. At the desired level, a transverse cut was made through one half of the spinal cord. In a separate experiment, small cuts were made at the ventral midline of the lumbar spinal cord. BDA crystals were inserted into the cut and allowed to diffuse into the cut axons (Supporting Information Fig. S1). Preparations were incubated overnight at room temperature in constantly oxygenated (95% O_2/5% CO_2) Ringer's Solution. Following incubation, spinal cords were fixed for 1–3 h in 4% PFA (Electron Microscopy Sciences) in phosphate-buffered saline (PBS) and then cryoprotected in 20% sucrose in PBS overnight. Spinal cords were sectioned transversely on a cryostat as 20 (at E12.5 and E14.5) or 30 (at P0) micrometer sections, which were mounted on a series of 10 slides.

Immunohistochemistry and Streptavidin-Biotin Histochemistry

Spinal cord sections on slides were subjected to streptavidin-biotin labeling and immunolabeling. Sections were first washed in PBS before being washed in PBS containing 0.1% Triton X (PBS-T). Slides were incubated in blocking solution (PBS containing 10% heat-inactivated normal goat serum (Invitrogen) and 0.1% Triton X) for 1 h at room temperature, and incubated overnight in anti-DsRed primary antibody (Clontech) at 4°C. The DsRed primary antibody can specifically recognize the tdTomato protein and was used to enhance and preserve the fluorescent signal in V3 INs. DyLight™594-conjugated Goat anti-Rabbit secondary antibodies (Jackson ImmunoResearch Laboratories) were diluted at 1:500. Biotin-linked Dextran Amine was labeled with Alexa Fluor 488-conjugated streptavidin (Jackson ImmunoResearch Laboratories, Inc.), diluted at 1:500, and added along with secondary antibodies. Sections were washed in PBS and cover-slipped with Dako fluorescent mounting medium.

Data Acquisition and Analysis

Images were obtained using a Zeiss Axiovert 200M fluorescence microscope or a Zeiss LSM 710 upright confocal microscope. TdTomato- and BDA-positive cells were mapped and counted in transverse spinal cord sections.

To determine V3 IN number at P0, we counted and mapped V3 INs in a series of transverse 30 μm sections in each region. In the lower thoracic region, we analyzed a total of 10 sections per animal, covering 1500 μm. In the upper lumbar region, we analyzed a total of 18 sections per animal, covering 2700 μm. Means of total counts were obtained from four *Sim1* mutant and four *Sim1* control spinal cords.

Cell density analysis was conducted using ImageJ and MATLAB. Contour maps of V3 INs were made by projecting all tdTomato-positive V3 INs from 12 random transverse 30 μm sections across lower thoracic and upper lumbar regions onto a single scaled half transverse section (Supporting Information Fig. S2A) and then using the *griddata* and *contourf* functions in MATLAB to generate the map with the log-transformed cell counts (Supporting Information Fig. S2B). Eight contour map images, four from control and four from mutant spinal cords, were subjected to principle component analysis (PCA) (Supporting Information Methods, Fig. S3).

In retrograde labeling experiments, BDA and tdTomato double positive cells were mapped and counted in Sim1 control and mutant animals at E12.5, E14.5, and P0. BDA application was unilateral (except specific indication in the text); thus, we identified four principal projection phenotypes: dIIN = descending ipsilateral, dCIN = descending contralateral, aIIN = ascending ipsilateral, aCIN = ascending contralateral (Eide et al., 1999). We counted each of these in 12 nonconsecutive 20 μm (for E12.5 and 14.5) and eight nonconsecutive 30 μm (for P0) sections within each 600 μm stretch of spinal cord, continuing until no more labeled cells were found. The histograms present average counts in each 600 μm stretch of various spinal cords.

Statistics

Cell counts in different V3 IN subgroups or of retrogradely labeled V3 INs were compared between $Sim1^{Cre/tauLacZ}$;*tdTom*, and $Sim1^{Cre/+}$;*tdTom* animals using a log-linear model. Briefly, the model fitted (natural) log-transformed counts Y to the linear model $\log(Y) = aX + b$, where X is an indicator variable taking on values 0 or 1 for $Sim1^{Cre/tauLacZ}$;*tdTom;* and control V3 INs, respectively. Hence, the expected values (E) for the two types are $E[\log(Y)$ given $X = 0] = b$ and $E[\log(Y)$ given $X = 1] = a + b$. The difference $E[\log(Y)$ given $X = 1] - E[\log(Y)$ given $X = 0]$ is, therefore, estimated by a. Transformation back to counts gives an

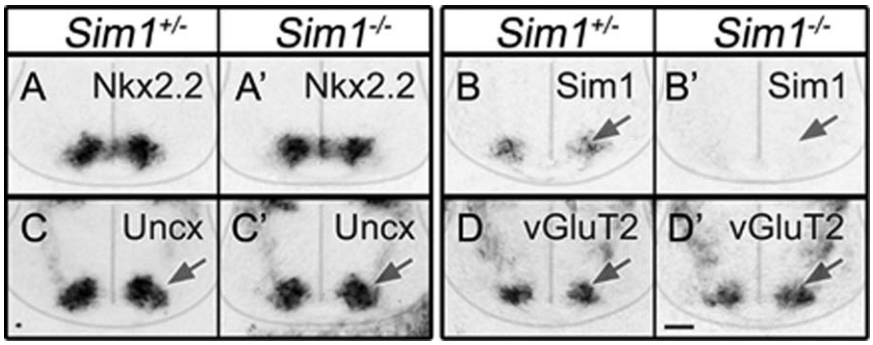

Figure 1 Loss of Sim1 does not change the identity of V3 INs. A–D: E11.5 spinal cord transverse sections hybridized with RNA probes against Nkx2.2 (A), Sim1 (B), Uncx (C), and vGluT2 (D) in heterozygous and *Sim1* mutant embryos. Scale bar, 25 μm.

estimate of the ratio $E[Y \text{ given } X = 1]/E[Y \text{ given } X = 0] = e^{a}$. The model provides a two-tailed test for the null hypothesis that the *Sim1 mutant /Sim1 control* count ratio is 1.

For the case of retrograde labeling by application of BDA to the midline, cell counts of BDA-labeled V3 INs were normalized against the total number of BDA-positive INs (i.e., observed counts divided by total). Statistical significance between the *Sim1* mutant and control groups was subsequently assessed via a *z*-test for comparing two proportions.

All counted data are presented as mean ± SD following the Poisson distribution. All statistical analysis was performed in MATLAB. $*p \leq 0.05$, $**p \leq 0.01$, $***p \leq 0.001$.

RESULTS

Sim1 Influences the Migration and Aggregation of V3 INs in the Mouse Spinal Cord

To assess the role of *Sim1* in the development of V3 INs, we generated a $Sim1^{Cre/tauLazZ}$;*tdTom* mouse (herein *Sim1* mutant), in which both *Sim1* alleles are disrupted by the insertion of Cre and tau-LacZ such that no functional Sim1 protein is produced (Zhang et al., 2008) [Fig. 1(B)]. *Sim1* heterozygotes ($Sim1^{Cre/+}$;*tdTom*) were used as control animals.

To determine if loss of Sim1 affected the generation of V3 INs, we analyzed the mRNA transcripts of the p3 progenitor marker Nkx2.2 [Fig. 1(A)], the postmitotic marker Sim1 [Fig. 1(B)] and the transcription factor Uncx [Fig. 1(C)] which is also expressed in newly born V3 neurons at E11.5 (Carcagno et al., 2014). Since V3 INs are excitatory, we also examined the expression of the vesicular glutamate transporter vGluT2 [Fig. 1(D)]. We found that with the exception of loss of expression of Sim1 in the mutant, control and *Sim1* mutant embryos displayed similar expression patterns of Nkx2.2, Uncx, and vGluT2 in the ventral spinal cord. This demonstrates that loss of Sim1 does not affect the early generation and differentiation of the spinal V3 IN population, indicating Sim1 plays primarily a role in the postmitotic development of the V3 INs.

The function and organization of neural circuits are different among segments from rostral to caudal spinal cord. We focused on lower thoracic and lumbar regions, which harbor the neuronal networks that control the movement of hind limbs, and assessed differentially the lower thoracic (T11–13), upper lumbar (L1–L3), and lower lumbar (L4–L6) regions (Fig. 2). No differences in the distribution and position of tdTomato-labeled V3 INs was seen at any of these levels in the mutant versus control mice up to E12.5 (Fig. 2(A,A″,B,B″)].

Examination at E14.5 revealed that the tdTomato-positive V3 INs had migrated away from their initial ventral position. In the lower thoracic and upper lumbar regions of control mice, we could identify distinct subgroups of tdTomato-positive V3 INs, in particular the ventral, intermediate, and dorsal subgroups, which tended to cluster separately [Fig. 2(C,C′)]. In the *Sim1* mutant mice, however, the tdTomato-positive V3 INs did not form such subgroups as distinctly as in controls, and we noted especially the lack of a prominent dorsal subgroup [Fig. 2(D,D′)]. Examination of the lower lumbar region (L4-L6) revealed only two main subgroups, a ventral and an intermediate, with no obvious dorsal subgroup in both mutant and control animals (compare panels C″ with D″). A differential distribution of V3 INs at different segments of the spinal cord was reported by our previous and others' studies (Francius et al., 2013, Borowska et al., 2013), which may be due to a differential development of spinal neurons along the rostrocaudal axis at different stages. Since we found clear differences in the dorsal and intermediate

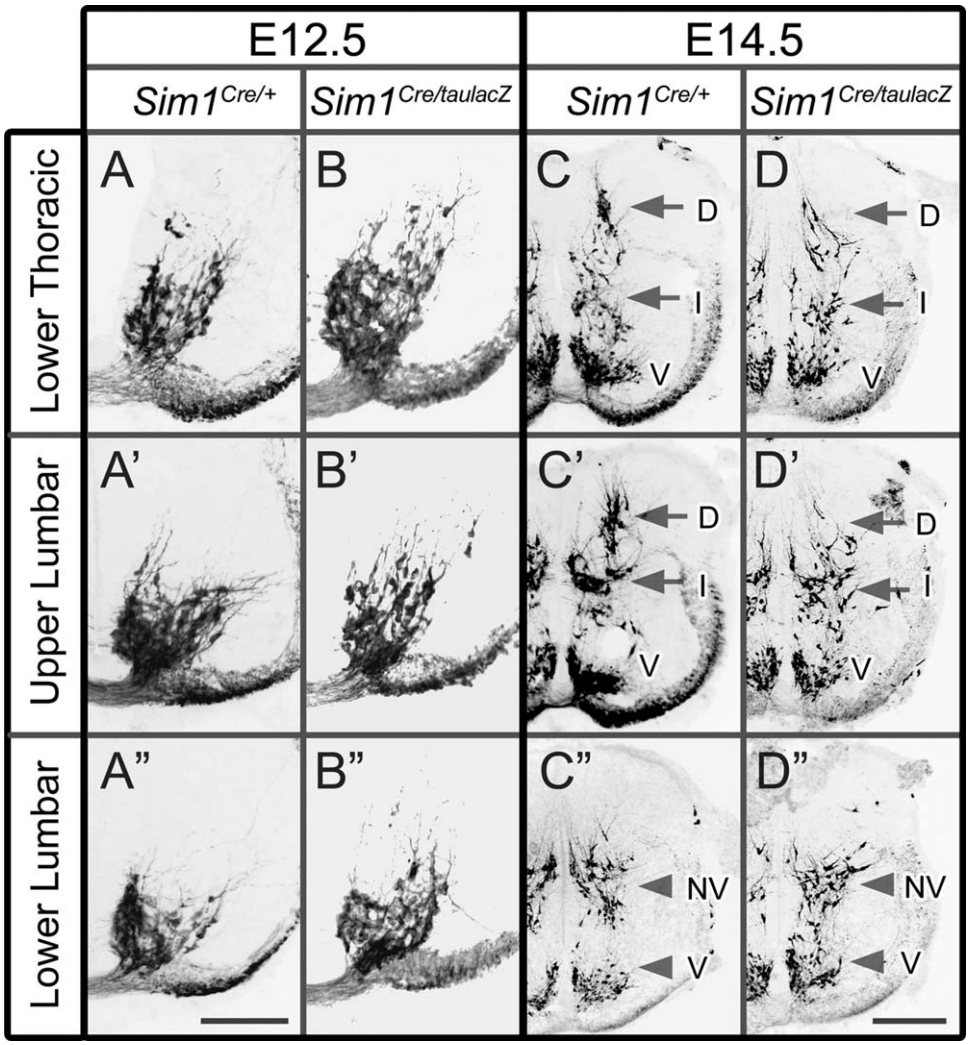

Figure 2 Sim1-deficient V3 INs show altered migration by E14.5. A, B: Transverse sections from E 12.5 *Sim1* control (*Sim1*$^{cre/+}$*;tdTom*, A,A″) and mutant (*Sim1*$^{cre/tauLacZ}$*;tdTom*, B,B″) spinal cords at lower thoracic (A and B), upper lumbar (A′ and B′) and lower lumbar (A″ and B″) regions. Scale bar = 100 μm. C,D: Transverse sections from E14.5 Sim1 control (C,C″) and Sim1 mutant (D,D″) spinal cord in lower thoracic (C,D), upper lumbar (C′,D′) and lower lumbar (C″,D″). V3 INs were visualized by tdTomato expression. Scale bar = 200 μm. D, dorsal; I, intermediate; V, ventral; NV, nonventral.

subgroups of V3 INs between and within control and mutant animals in the lower thoracic and upper lumbar regions, the remainder of our study focuses on these regions.

We next examined the locations of V3 INs in the spinal cords of newborn pups, a stage when tdTomato-positive V3 INs have attained positions along the dorsoventral axis similar to those seen in the mature spinal cord (Borowska et al., 2013). In lower thoracic and upper lumbar segments, V3 INs were found in the deep dorsal horn and in almost all ventral horn regions, mainly at medial locations. V3 INs in control mice tended to group together at different locations along the dorsoventral axis [Fig. 3(A,A′)]. To describe the distribution of the V3 INs in neonates more accurately, we defined three subpopulations: a major subgroup of ventral V3 INs located in lamina VIII, an intermediate subgroup located in laminae VI, VII, and X, and a dorsal subgroup located in lamina V (occasionally also in lamina IV) (Zhang et al., 2008; Borowska et al., 2013). Similar to what we observed at E14.5, ventral and dorsal V3 INs were well defined into coherent subgroups, whereas the distribution of intermediate V3s appeared less organized and varied among different segments [Fig. 3(A,A′)]. In the *Sim1* mutant [Fig. 3(B,B′)], the separation of the different V3 subgroups become less distinct, and there appeared in particular

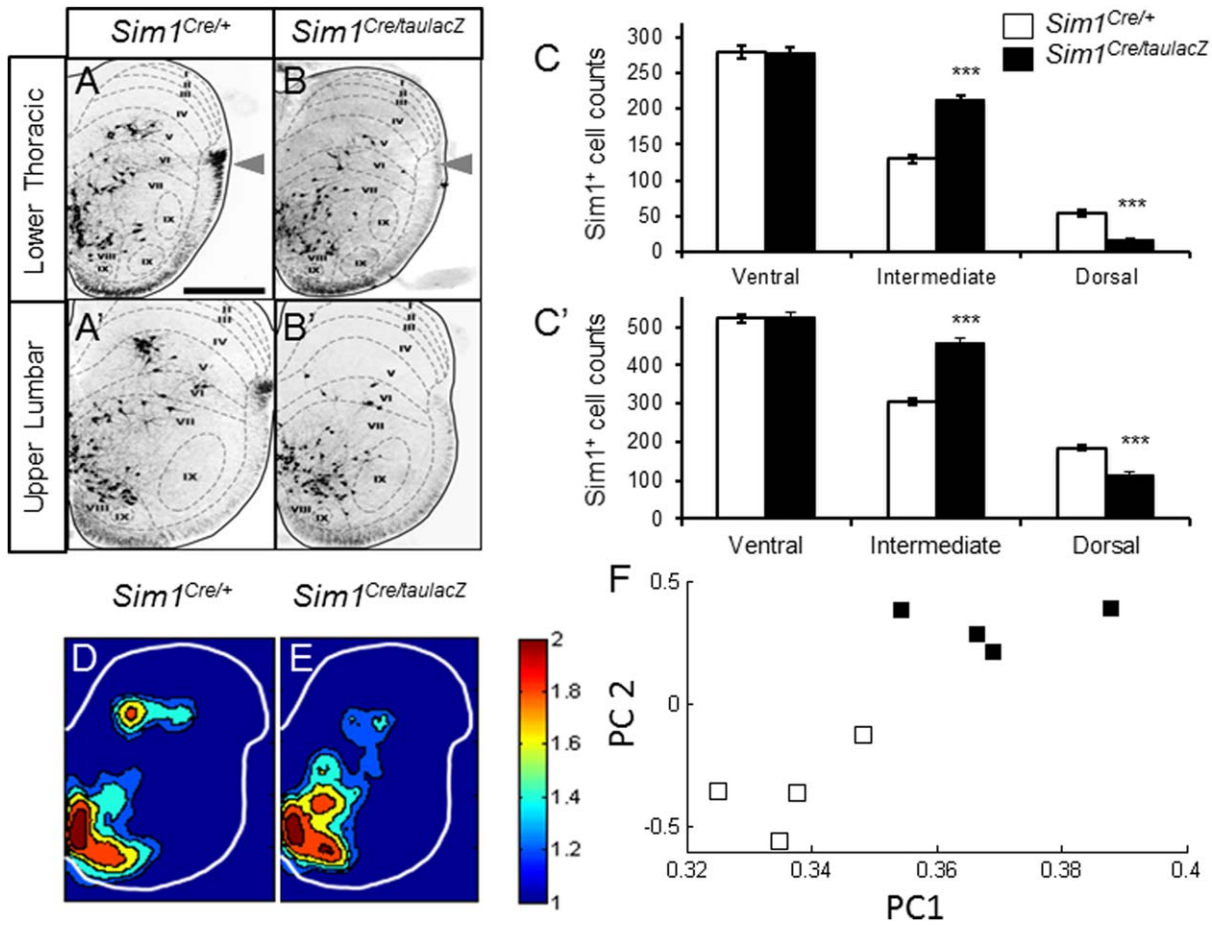

Figure 3 *Sim1* mutant V3 INs show altered distribution pattern of different subgroups at P0. A, B: Transverse sections from P0 Sim1 control (*Sim1*$^{cre/+}$;*tdTom*, A,A′) and mutant (*Sim1*$^{cre/tauLacZ}$;*tdTom*, B,B′) spinal cords at lower thoracic (A and B) and upper lumbar (A′ and B′) regions. Scale bar = 100 μm. Arrowhead: tdTomato positive axon tracts in the lateral-dorsal funicular. The postulated Rexed's laminae are outlined (the dashed lines) on each transverse section to indicate the relative position V3 INs. C: Number of V3 INs in Sim1 control (white bar, $n = 4$) and mutant (black bar, $n = 4$) spinal cords classified according to their location (Ventral, Intermediate or Dorsal) at lower thoracic (C) and higher lumbar (C′) segments. ***: $p < 0.001$. D, E: Representative contour maps of tdTom$^+$ (V3) neurons in *Sim1* control (D) and mutant (E) spinal cords. The color bar indicates the log-transformed cell counts from high (red) to low (blue). F: The scatter plot of the PC1 coordinated with the PC2 values of the contour images from *Sim1* control (white) and mutant (black) spinal cords.

to be much fewer dorsal V3 INs in lamina V [Fig. 3(B,B′)].

To quantify V3 IN number in different subgroups at P0, we analyzed a series of transverse sections through the lower thoracic and upper lumbar cords. At lower thoracic region, no differences in cell number of ventral V3 INs were seen between the control and *Sim1* mutant mice [mutant = 278.5 ± 8.34 cells, $n = 4$, vs. control = 279.7 ± 8.36 $n = 4$, Fig. 3(C,C′), left columns]. However, a 70% reduction in the number of V3 INs in the dorsal subgroup in the mutant mice (mutant = 16 ± 2 cells, $n = 4$, vs. control = 53.8 ± 3.7 cells, $n = 4$, $p < 0.001$) and an increase of 39% in the number of V3 INs in the intermediate subgroup (mutant = 212.5 ± 7.3 cells, $n = 4$, vs. control = 129.8 ± 5.7 cells, $n = 4$, $p < 0.001$) [Fig. 3(C′)]. The upper lumbar region showed a similar pattern, namely 38% fewer V3 INs in the dorsal subgroup (mutant = 114.6 ± 5.4 cells, $n = 5$, vs. control = 183.8 ± 6.8 cells, $n = 4$, $p < 0.001$) and 33% more V3 INs in the intermediate subgroup (mutant = 459.4 ± 10.7 cells, $n = 5$, vs. control = 306.5 ± 8.8 cells, $n = 4$, $p < 0.001$), while no change was apparent in the ventral subgroup (mutant = 525.8 ± 11.4

cells, $n = 4$, vs. control = 522.5 ± 11.4 cells). Interestingly, there was a small (8–9%) but significant increase in the total number of V3 INs in the *Sim1* mutant (lower thoracic: mutant = 510.5 ± 11.3 cells, $n = 4$, vs. control = 464.8 ± 10.8 cells, $n = 4$, $p = 0.0034$; upper lumbar: mutant = 1099.8 ± 14.8 cells, $n = 5$, vs. control = 1012.8 ± 15.9 cells, $n = 4$, $p < 0.001$).

To better understand the changes in the distribution pattern of V3 INs in the *Sim1* mutant, we conducted additional analysis of cell density. Contour maps of the tdTomato positive V3 INs in control and mutant spinal cords showed a similar density distribution in the ventral horn region, but distinct density distributions in the intermediate and dorsal regions [Fig. 3(D,E)]. In particular, the dorsal subgroup was smaller, the intermediate subgroup larger, and the separation between these two groups was diminished [Fig. 3(D,E)]. To quantify these changes, we conducted PCA of the contour maps of four control and four mutant spinal cords (Supporting Information Fig. S3). The first two principle components (PC1 and PC2) captured more than 81% of the total variance in the eight images and clearly separated the mutant from the control spinal cords [Fig. 3(F)]. ANOVA was conducted on each component separately. Results indicated that the mean PC1 and PC2 for mutant and control are significantly different ($p = 0.007$ for PC1, $p < 0.001$ for PC2), thus, indicating a significant difference of the distribution patterns in mutant and control V3 INs.

Overall, these results clearly demonstrate that mutant V3 INs do not reach the deep dorsal horn properly and that the organization of V3 INs in the dorsal and intermediate regions is compromised.

Development of Axonal Projections in Sim1 Control Spinal Cords

Projections from the V3 INs are predominantly commissural (Zhang et al., 2008). However, a careful analysis of the V3 IN axon projections during development has not been done. To characterize the projection pattern during normal development, we performed retrograde labeling studies following unilateral applications of BDA at L1 in control spinal cords at E12.5, E14.5, and P0 (Fig. 4). We counted all double labeled (BDA-positive/tdTomato-positive) cells rostral and caudal to the injection site to identify all ascending and descending ipsilateral and commissural V3 INs. We detected BDA/tdTomato double labeled V3 INs at all ages examined [Fig 4(A,E,I)]. At E12.5, double labeled INs were predominantly descending ipsilateral INs (dIINs; 81%), with descending contralateral (dCINs; 9%) and ascending contralateral (aCINs; 10%) comprising a minority of cells [Fig. 4(A–D)]. We observed no ascending ipsilateral V3 INs (aIINs). Note that all tdTomato-positive cells at this stage were located in the ventral region of the spinal cord [Fig. 4(D)].

By E14.5, commissural tdTomato-positive V3 INs became prevalent, with the number of aCINs (49%) and dCINs (25%) together exceeding that of dIINs (25%) by nearly threefold. A few aIINs (1%) also appeared [Fig. 4(E–H)]. The descending tdTomato-positive V3 INs were clustered in the ventromedial region of the spinal cord, whereas ascending tdTomato-positive V3 INs contributed to all three V3 IN subgroups [Fig. 4(H)].

By P0, commissural tdTomato-positive V3 INs became predominant, comprising 97% of the total number counted [Fig. 4(I–L)]. aCINs remained the largest subpopulation (64%), with dCINs making up 33%, and aIINs and dIINs together comprising only 3%. At P0, the distribution of different projection phenotypes resembled that seen at E14.5: descending tdTomato-positive V3 INs were located predominantly in the most ventral subgroup, whereas ascending tdTomato-positive V3 INs were distributed among all three V3 IN subgroups [Fig. 4(L)].

Sim1 Regulates the Contralateral Trajectory of V3 IN Commissural Axons

Sim1 reportedly functions in axon guidance in the hypothalamus and other regions in the CNS. (Marion et al., 2005; Schweitzer et al., 2013). Interestingly, we observed that a tdTomato-positive axon tract located in the dorsal region of the lateral funiculus was greatly decreased in *Sim1* mutants [Fig. 3(A,B); arrowheads], suggesting that axon development was altered by the loss of *Sim1* in Sim1 expressing neurons. To assess whether Sim1 is important for the projections of V3 INs, we applied BDA at L1 in *Sim1* mutant and control spinal cords, and quantified the number of BDA/tdTomato positive INs rostral and caudal to the injection site.

At E14.5 (Fig. 5), we detected BDA/tdTomato double-labeled V3 INs contralateral to the BDA application site in both mutant and control spinal cords [Fig. 5(A–F)]. Assessment of the dorsoventral distribution of tdTomato-positive V3 INs labeled retrogradely from L1 revealed a lack of BDA-labeled dorsal V3 INs in mutant spinal cords, consistent with the migration defects described above [Fig. 5(G,H)]. The axons of mutant and control tdTomato-positive V3 INs projected comparable distances from L1, however, the number of tdTomato-positive V3 CINs

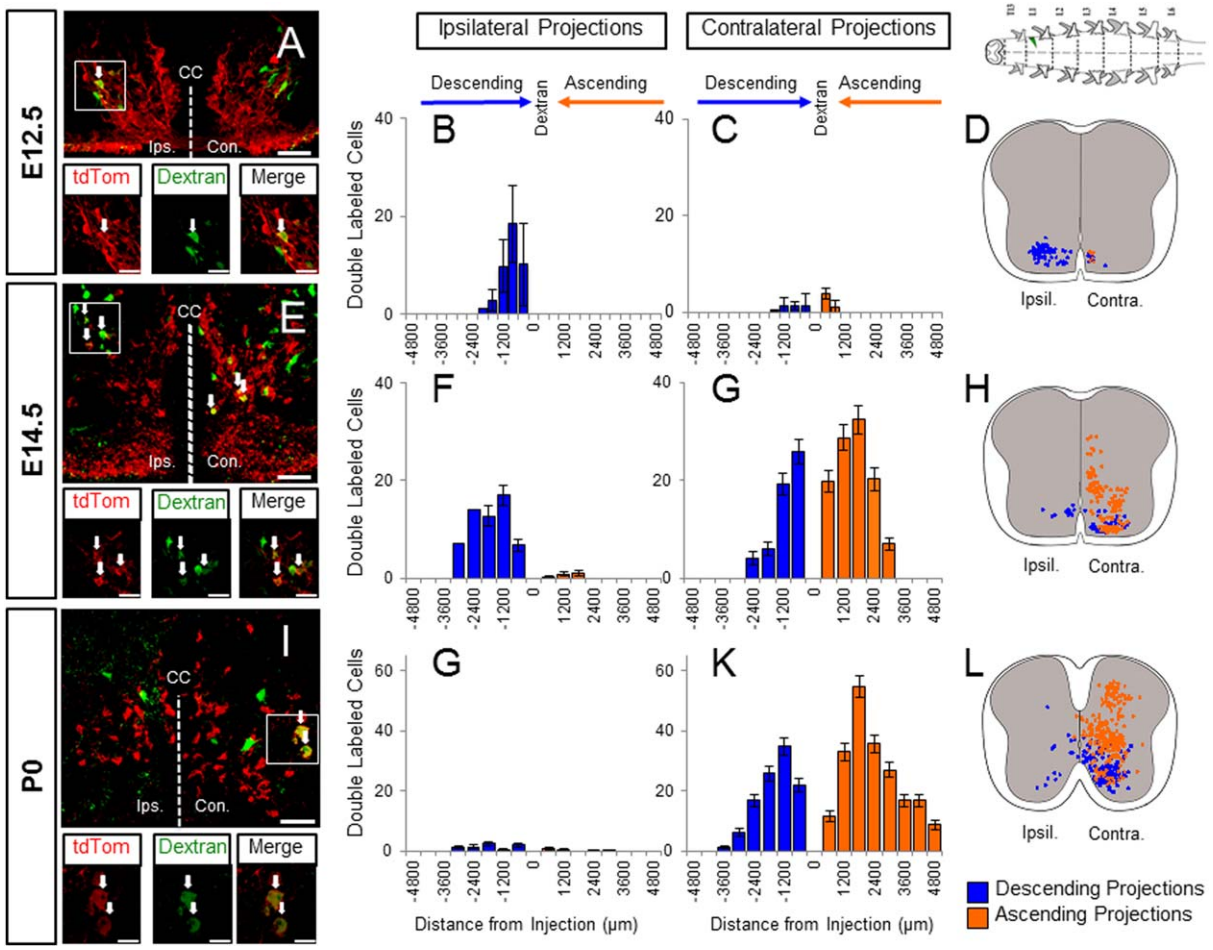

Figure 4 Axonal projections of V3 INs during development. A–D: Projection profiles of V3 INs at E12.5. TdTom (red) and BDA (green) double-labeled V3 INs were detected in transverse sections (A). Histograms ($n = 4$) show the number of tdTom/BDA double-labeled V3 INs projecting ipsilaterally (B) or contralaterally (C) to BDA application site. 0 on the *X*-axis (approximately L1) marks tracer application site. Negative numbers represent distance of the position of soma of BDA^+ neuron rostral to the application site (Descending projection, Blue), and positive numbers indicate distances caudal to that injection site (Ascending neurons, Orange). D: position of soma of V3 IN in transverse sections that project caudally (blue) or rostrally (orange). Schematic spinal cord indicates the application site of BDA (green) at L1 region. E–H: Projection profiles of V3 INs at E14.5. E: transverse section of the lumbar spinal cord with double-labeled V3 INs. F, G : Histograms ($n = 4$) of $tdTom^+/BDA^+$ V3 INs projecting ipsilateral (F) or contralateral (G) axons, both classified as descending (blue) or ascending (orange). H: the approximate soma positions of BDA^+ V3 INs. I–L: Projection profiles of V3 INs at P0. I: transverse section of the lumbar spinal cord with double-labeled V3 INs. G,K : Histograms ($n = 4$) of tdTom/BDA double-labeled V3 INs that project caudally or rostrally and locate ipsilateral (G) or contralateral (K) to BDA application site (L1). L: soma position of V3 INs that project caudally (blue) or rostrally (orange). Scale bar = 50 μm for large images, 25 μm for higher magnification smaller images.

decreased in the mutant spinal cord, especially those with short-range axons [Fig. 5(I,J)]. The number of dCINs and aCINs projecting to L1 in mutant cords decreased (dCINs: control = 60.2 ± 3.5, $n = 5$; mutant = 45.3 ± 3.9, $n = 3$; $p = 0.006$; aCINs: control = 118 ± 4.9, $n = 5$; mutant = 78.7 ± 5.12, $n = 3$; $p < 0.001$) [Fig. 5(K)]. This difference is unlikely to be due to other factors such as tissue health, since there was no significant difference in the number or projection distances of the ipsilaterally projecting tdTomato-positive V3 INs between the mutant and control mice (data not shown).

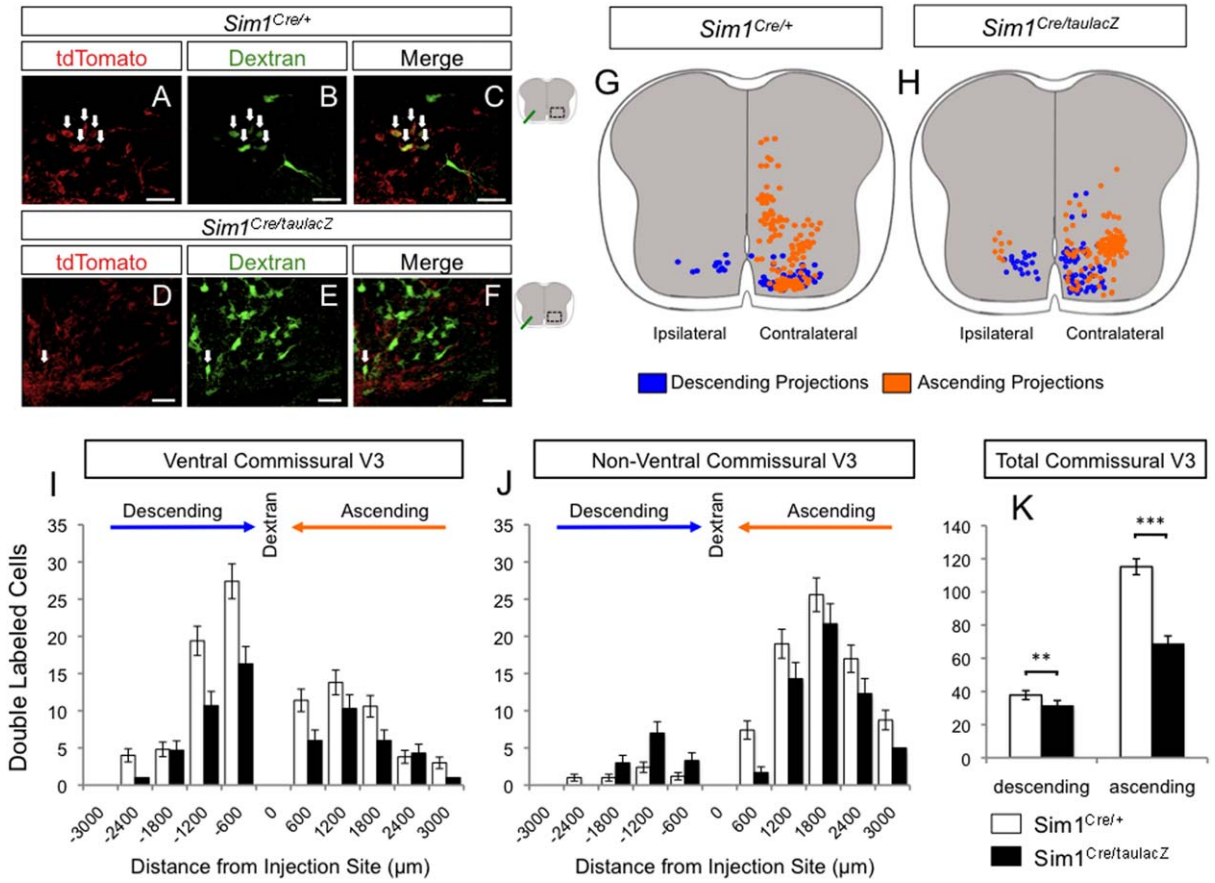

Figure 5 Sim1 is critical for proper projection of V3 axons at E 14.5. A–F: tdTom (red) and BDA (green) labeled V3 INs were detected in transverse sections of *Sim1* control (A–C) and mutant (D–F) spinal cords. Arrows indicate double-labeled cells. Scale bar = 50 μm. G, H: The position of V3 somas were mapped on transverse sections and marked according to their axonal projection (descending, blue or ascending, orange) in *Sim1* control (G) and mutant (H) spinal cords. I, J: Histograms of distribution of tdTom/BDA double-labeled cells that project contralaterally (commissural V3s) and are located in ventral regions (I) or at intermediate-dorsal positions (Nonventral, J). *Sim1* mutant (black, $n = 4$) and control (white, $n = 4$) spinal cords. K: The comparison of the total number of V3 dCINs and aCINs between mutant (black, $n = 4$) and control (white, $n = 4$) cords (K). $^{**}p < 0.01$; $^{***}p < 0.001$. Error bars show Poisson rate confidence intervals.

We observed similar phenotypes at P0: BDA-labeled V3 INs were present in all spinal cords examined [Fig. 6(A–F)], but there was a lack of dorsal V3 CINs and a substantial decrease in the number of ventral V3 aCINs projecting to L1 from all levels in the *Sim1* mutant spinal cords [Fig. 6(G,H)]. We next assessed the dorsoventral distribution of V3 INs labeled from L1, and observed a lack of BDA-labeled V3 INs in the dorsal region and a substantial decrease in the number of ventral V3 aCINs in the mutant [Fig. 6(G,H)]. The decrease in the number of double labeled V3 INs was seen at all levels of the spinal cord assessed, although mutant and control V3 INs still projected comparable distances from L1, except for the very small population of nonventral (intermediate + dorsal) dCINs [Fig. 6(I,J)]. Statistical analysis showed that the number of mutant V3 aCINs was reduced by 47% (control = 194.7 ± 7.0, $n = 4$; mutant = 91.8 ± 4.8, $n = 4$; $p < 0.001$) and the number of mutant V3 dCINs was reduced by 45% (control = 107 ± 5.2, $n = 4$; mutant = 47.8 ± 3.4, $n = 4$; $p < 0.001$) [Fig. 6(K)]. Taken together, these results show that Sim1 is crucial for V3 INs to establish their proper contralateral projection patterns.

To determine whether these axon projection defects were specific to the upper lumbar region, we performed BDA labeling at L5 at P0 (Fig. 7). Similar to the case for V3 INs projecting to L1, the number of ventral V3 aCINs and dCINs projecting to L5 in the mutant animals decreased relative to controls

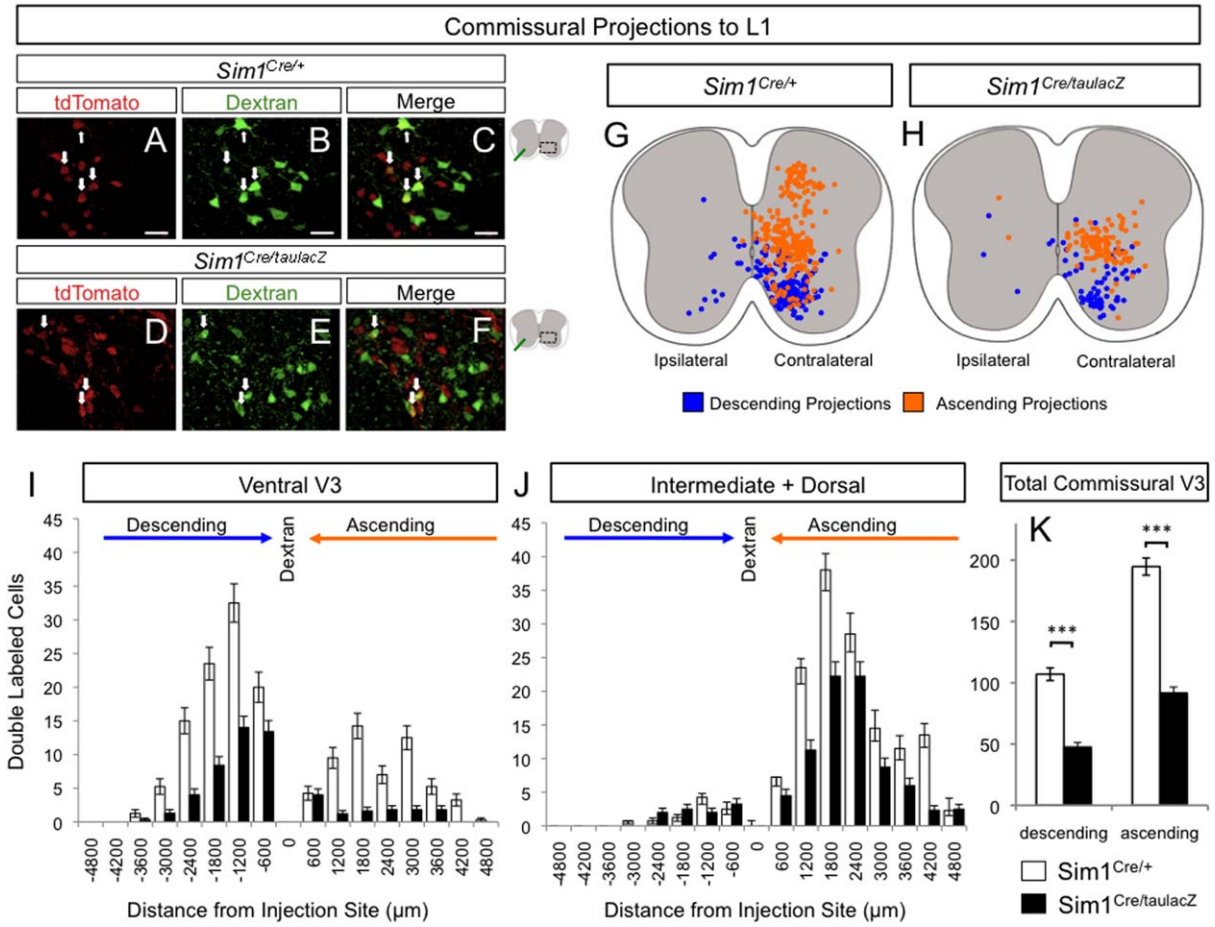

Figure 6 *Sim1* mutant V3 INs show decreased axonal projections to L1 at P0. A–F: TdTom (red) and BDA (green) labeled cells were detected in transverse sections of *Sim1* control (A–C) and mutant (D–F) P0 spinal cords. Arrows indicate double-labeled cells. Scale bar = 50 μm. G, H: The soma position of V3 INs that project caudally (blue) or rostrally (orange) to the dextran application site at the L1 segment in *Sim1* control (G) and mutant (H) spinal cords. I, J: Histograms of tdTom/BDA double-labeled ventral (I) and intermediate-dorsal (Nonventral, J) V3 INs projected contralaterally to BDA application site (L1) from *Sim1* mutant (black, $n = 4$) and control (white, $n = 4$) spinal cord. K: Comparison of the total number of V3 dCINs and aCINs between mutant (black, $n = 4$) and control (white, $n = 4$) cords. **: $p < 0.01$; ***: $p < 0.001$. Error bars show Poisson rate confidence intervals.

[Fig. 7(A–C)]. Nonventral BDA labeled V3s did not appear very different between mutant and control animals, however [Fig. 7(D)]. Taken as a whole (ventral and nonventral combined), V3 dCINs decreased by 52% (control = 99.5 ± 5.0, $n = 5$; mutant = 51.3 ± 4.1, $n = 3$; $p = 3.08$ E − 12), while there was no significant change in the number of V3 aCINs [Fig. 7(E)]. We note that the V3 aCINs labeled from L5 are mainly from the sacral region, which did not have a dorsal population and, therefore, did not exhibit the same migration defects (data not shown).

Given these observed deficits in the V3 CIN axon projections to L1 and L5 in the mutant spinal cord, we asked whether this phenotype might be due to fewer V3 INs projecting axons across the midline. We observed no obvious difference in the thickness of the tdTomato-positive axon bundle in the ventral commissure in control versus mutant spinal cords [Fig. 8(A,B)]. We applied BDA to the midline of the upper lumbar region of mutant and control spinal cords at P0 [Fig. 8(C,D)] to assess the total commissural V3 INs. The proportion of tdTomato/BDA doubled-labeled V3 INs, which made up around 10% of all crossing axons, did not differ between *Sim1* mutant ($n = 3$) and control ($n = 4$) spinal cords [Fig. 8(E)]. This suggests that the loss of Sim1 does not alter midline crossing, but rather affects the longitudinal growth of axons once they have crossed the midline.

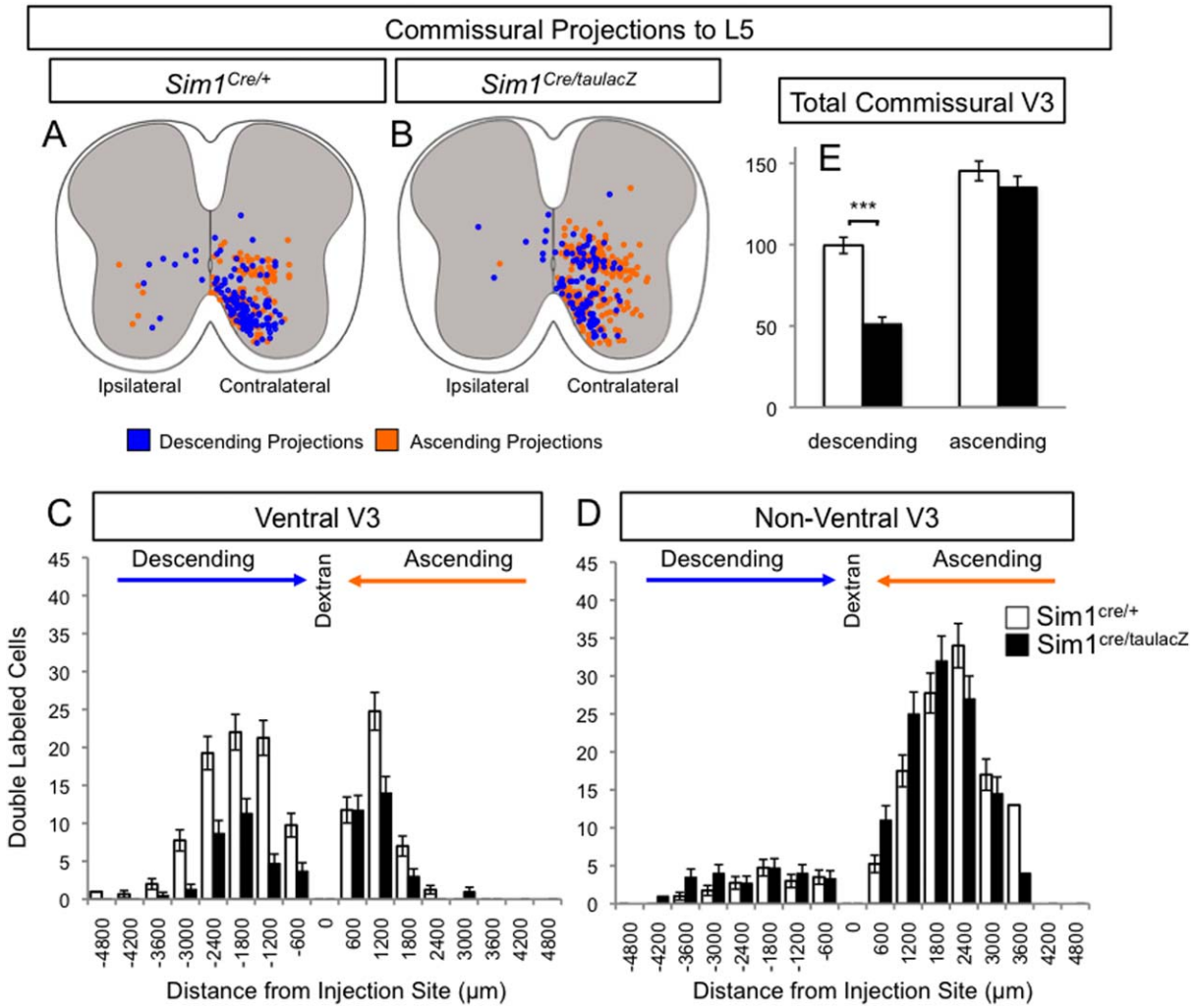

Figure 7 *Sim1* mutant V3 INs show altered axonal projections to L5 at P0. A, B: The approximate dorsoventral soma position of V3 INs that project caudally (blue) or rostrally (orange) to L5 (the dextran application site) from *Sim1* control (A) and mutant (B) spinal cords. C, D: Histograms of tdTom/BDA double-labeled ventral (C) and Nonventral (D) V3 INs projected contralaterally to BDA application site (L5) from *Sim1* mutant (black, $n = 3$) and control (white, $n = 4$) spinal cord. E: Comparison of the total number of V3 dCINs and aCINs between mutant (black, $n = 3$) and control (white, $n = 4$) cords. ***: $p < 0.001$. Error bars show Poisson rate confidence intervals.

DISCUSSION

To assess the function of the transcription factor Sim1 in developing spinal V3 INs, we systematically characterized the localization and axonal projection profile of V3 INs during the embryonic and perinatal periods. We compared these features in V3 INs expressing Sim1 and in V3 INs in which Sim1 expression was genetically ablated. Our findings demonstrate that Sim1 is necessary for establishing the proper positional topography of V3 INs and regulates the contralateral longitudinal projection of V3 IN commissural axons.

Postmitotic Development of V3 INs

V3 INs emerge from the p3 progenitor domain of the developing neural tube between E9.5 and E11.5 (Briscoe et al., 1999; Zhang et al., 2008; Carcagno et al., 2014). As early as E12.5, a dorsal and lateral migratory stream of V3 INs can be observed. At E14.5, V3 INs in the lower thoracic and upper lumbar region of control embryos continue to migrate dorsolaterally and separate into subgroups that attain their final positions by P0. Based on their anatomical locations, we have defined these subgroups as ventral, intermediate, and dorsal. These subgroups remain anatomically distinct after postnatal development in

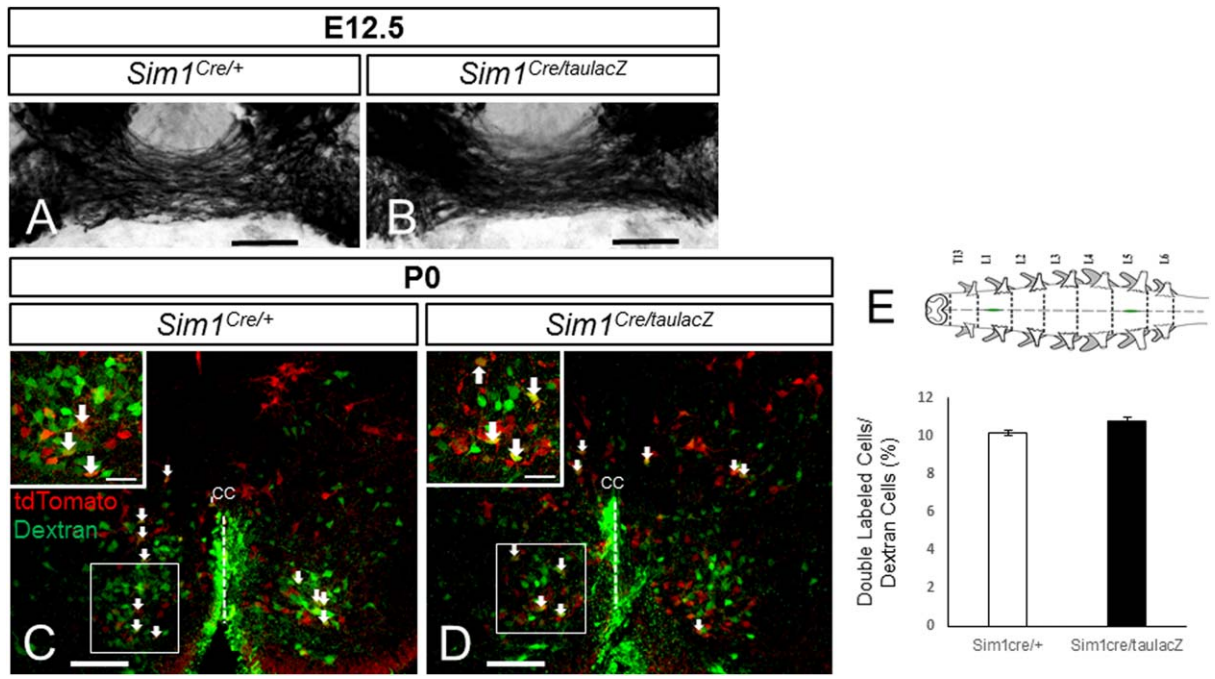

Figure 8 *Sim1* mutant V3 INs display normal midline crossing. A, B: Ventral commissures of V3 INs from 30 μm transverse sections of *Sim1* control (A) and mutant (B) spinal cords at E12.5, enlarged to show tdTomato positive projections across the ventral midline. Scale bar = 100 μm. C, D: BDA and tdTomato double-labeled V3 INs from transverse sections of *Sim1* control (C) and mutant (D) spinal cords subjected to midline dextran application. Scale bar = 100 μm for large images, 40 μm for higher magnification images (inset). CC, central canal; Arrows point double-labeled cells. E: Quantification indicates no significant differences in the number of V3 INs across the midline between mutant (black, $n = 3$) and control (white, $n = 4$) spinal cords.

the mature spinal cord (Borowska et al., 2013). Functionally, V3 INs in the different subgroups likely participate differentially in spinal networks, as they exhibit distinct electrophysiological and morphological properties (Borowska et al., 2013).

The dorsal-lateral migration trajectory exhibited by V3 INs is not common in the spinal cord, where most INs migrate ventrally and/or laterally from the midline (Moran-Rivard et al., 2001; Saueressig et al., 1999; Lundfald et al., 2007). However, sympathetic preganglionic neurons also undergo dorsolateral migration during postmitotic development, an activity mediated in part by Reelin-related pathways (Yip et al., 2009).

Although V3 INs are predominantly commissural INs (CINs), a small contingent of ipsilaterally projecting V3 INs (V3 IINs) is also present in postnatal spinal cords (Zhang et al., 2008). Here, we further confirmed that V3 IINs are present during early embryonic stages, and that they are predominantly dIINs. Indeed, our retrograde labeling studies in the E12.5 mouse spinal cord revealed that most labeled V3 INs were dIINs. The fact that we observed a substantial number of V3 IN axons in the ventral commissure as early as E11.5 (Zhang et al., 2008) without detecting many retrogradely labeled V3 CINs at E12.5, suggests a delay in the longitudinal growth of commissural axons after midline-crossing. V3 dIINs were still detected at E14.5 and P0; however, the proportion and total number of V3 IINs had decreased by birth. One explanation for our observation of fewer V3 IINs at P0 may be that during development the V3 dIIN axons fail to elongate as fast as the spinal cord grows longitudinally (Nissen et al., 2005), as has been seen for certain populations of central sensory axons (Eide and Glover, 1995), or that the axons retract, becoming too short to be detected by our retrograde labeling procedure. However, we cannot rule out the possibility that some V3 IINs die or that they lose an ipsilateral branch of an originally bifurcated axon, and these possibilities remain to be tested.

Although the dIIN population of V3 INs changed during development, the V3 CIN projection profile at E14.5 was similar to the profile of CINs previously described (Nissen et al., 2005), which comprises both

dCINs and aCINs. More specifically, all dorsal and most intermediate V3 CINs were aCINs, whereas ventral V3 CINs comprised both aCINs and dCINs. These projection patterns were maintained until at least P0.

Sim1 Function in the Spinal Cord

Sim1, as a member of the bHLH/PAS family, plays an important role in regulating the embryonic development and postnatal functions of many cell types including neurons in the CNS (Kewley et al., 2004). In particular, Sim1 is critical for the proper formation and organization of the mamillothalamic and mamillotegmental tracts in the mouse (Marion et al., 2005) and of the thalamospinal tracts in zebrafish (Schweitzer et al., 2013). In addition, Sim1 has been implicated in regulating neuronal migration within the supraoptic and paraventricular nuclei in the mouse hypothalamus (Xu and Fan, 2007). Our current experiments indicate that *Sim1* regulates the topological positioning of V3 spinal INs in the lower thoracic and upper lumbar regions as well as the growth of their axons.

In *Sim1* mutants, V3 INs are still generated in the ventromedial region from the p3 progenitor domain of the developing spinal cord, and they maintain a predominantly excitatory (glutamatergic), commissural phenotype as in the wild type. Although our quantification revealed that the total numbers of V3 INs were slightly greater in the Sim1 mutants, which may reflect a role for Sim1 in the regulation of apoptosis (Xu and Fan, 2007), the V3 INs in the *Sim1* mutant were abnormally distributed, with increased numbers of intermediate V3 INs coming at the expense of the dorsal V3 subgroup. Correlated with these changes, the dorsal and intermediate subgroups of V3 INs were loosely organized in the *Sim1* mutant spinal cord, suggesting that Sim1 is important for the migration and topological organization of V3 INs. Although the change in the V3 dorsoventral distribution may be due to a delay in migration of V3 INs in the *Sim1* mutant, it is more likely that Sim1 is an important regulator of signaling by guidance molecules. Xu and Fan (2007) revealed that Plexin C1 could be a downstream molecular factor regulated by Sim1 in the hypothalamus. The precise expression pattern of Plexin C1 has not been described in the developing mouse spinal cord, but it would not be surprising if Plexins, Neuropilins, and their ligands the Semaphorins, many of which are expressed in the spinal cord (Raper, 2000; Zou et al., 2000), are involved in the aggregation and migration defects seen in *Sim1* mutant V3 INs.

In addition to V3 IN migration defects, *Sim1* mutant mice exhibited aberrant projections of commissural axons, with a significant decrease in the number of contralaterally-projecting V3 INs. This was surprising given that there were few defects in the ability of V3 CIN axons to cross the midline, suggesting that the defects were rather related to the projection once crossed.

One explanation for this observation is that Sim1 may regulate the expression of a guidance receptor, as has been demonstrated for many bHLH transcription factors (Meijer et al., 2012). Interestingly, Sim1 has been shown to regulate the expression of Rig-1/Robo3, and signaling through the Robo/Slit complex governs axon guidance in neurons in the mouse mammillary body and zebrafish hypothalamus (Marion et al., 2005; Schweitzer et al., 2013). In both cases, loss of Sim1 leads to the upregulation of Robo3, which changes the sensitivity of the mutant neurons to repellent proteins and directs the mutant axons aberrantly towards the midline. In the spinal cord, many commissural axons upregulate Rig-1/Robo3 prior to midline crossing. On crossing they then upregulate the expression of Robo1 and Robo2, initiating a repulsive cue (Mambetisaeva et al., 2005; Reeber et al., 2008; Jaworski et al., 2010). In our current study, we observed no obvious deficiency in V3 IN axon midline crossing, but rather clear defects in their subsequent longitudinal extension. Thus, Sim1 may regulate Slit-Robo signaling in V3 IN axons after midline crossing directly, or affect Slit-Robo dependent nonsense-mediated mRNA decay (NMD). Recently, Colak et al. (2013) showed that Robo3.2 in the growth cone is regulated by activation of NMD pathways in the floor plate, and that this in turn affects the projection of commissural axons after midline crossing. Other guidance factors may also be involved in directing the longitudinal extension of V3 IN axons after midline crossing, including Netrin, Wnts, and Shh, all of which have differential distributions along the longitudinal axis (Lyuksyutova et al., 2003; Bourikas et al., 2005; Okada, 2006; Domanitskaya et al., 2010; Yam et al., 2013). These possibilities remain to be tested.

In summary, our current study has systematically studied the spatial and temporal development of V3 INs in the lower thoracic and upper lumbar spinal cord, and the role for Sim1 during these processes. Originating from the most ventral progenitor domain, V3 INs migrate into three distinct subgroups along the dorsoventral axis. Sim1 is a critical factor necessary for the development of these subgroups and the appropriate targeting of their axonal projections. Loss of Sim1 leads to a loss of dorsal V3 INs with an

increase in the number of intermediate V3 INs. At the same time, longitudinal extension of the contralateral axons of V3 INs is reduced. These Sim1-regulated events may involve molecular pathways that function after V3 IN axons cross the midline, and may be crucial for V3 INs to correctly integrate into spinal networks and to help produce robust and balanced motor outputs.

J.P.F is a Tier 2 Canada Research Chair in Mechanisms of Brain Repair. We thank Dr. Martyn Goulding for generously providing *Sim1*$^{Cre/+}$*;tdTom* and *Sim1*^{tauLacZ} mice.

REFERENCES

Borowska J, Jones C, Zhang H, Blacklaws J, Goulding M, Zhang Y. 2013. Functional subpopulations of V3 interneurons in the mature mouse spinal cord. J Neurosci 33: 18553–18565.

Bourikas D, Pekarik V, Baeriswyl T, Grunditz A, Sadhu R, Nardó M, Stoeckli E. 2005. Sonic hedgehog guides commissural axons along the longitudinal axis of the spinal cord. Nat Neurosci 8:297–304.

Briscoe J, Sussel L, Serup, P, Hartigan-O'Connor D, Jessell TM, Rubenstein JL, Ericson J. 1999. Homeobox gene Nkx2.2 and specification of neuronal identity by graded sonic hedgehog signalling. Nature 398:622–627.

Carcagno AL, Di Bella DJ, Goulding M, Guillemot F, Lanuza GM. 2014. Neurogenin3 restricts serotonergic neuron differentiation to the hindbrain. J Neurosci 34: 15223–15233.

Colak D, Ji S, Porse B, Jaffrey S. 2013. Regulation of axon guidance by compartmentalized nonsense-mediated mRNA decay. Cell 153:1252–1265.

Crone S, Quinlan K, Zagoraiou L, Droho S, Restrepo C, Lundfald L, Sharma K. 2008. Genetic ablation of V2a ipsilateral interneurons disrupts left-right locomotor coordination in mammalian spinal cord. Neuron 60:70–83.

Domanitskaya E, Wacker A, Mauti O, Baeriswyl T, Esteve P, Bovolenta P, Stoeckli E. 2010. Sonic hedgehog guides post-crossing commissural axons both directly and indirectly by regulating wnt activity. J Neurosci 30:11167–11176.

Eide AL, Glover JC. 1995. The development of the longitudinal projection patterns of lumbar primary sensory afferents in the chicken embryo. J Comp Neurol 353:247–259.

Eide AL, Glover JC, Kjaerulff O, Kiehn O. 1999. Characterization of commissural interneurons in the lumbar region of the neonatal rat spinal cord. J Comp Neurol 403:332–345.

Francius C, Harris A, Rucchin V, Hendricks TJ, Stam FJ, Barber M, Kurek D, et al. 2013. Identification of multiple subsets of ventral interneurons and differential distribution along the rostrocaudal axis of the developing spinal cord. PLoS One 8:e70325.

Glover JC. 1995. Retrograde and anterograde axonal tracing with fluorescent dextrans in the embryonic nervous system. Neurosci Protoc 30:1–13.

Gosgnach S, Lanuza GM, Butt SJB, Saueressig H, Zhang Y, Velazquez T, Riethmacher D, et al. 2006. V1 spinal neurons regulate the speed of vertebrate locomotor outputs. Nature 440:215–219.

Goulding M. 2009. Circuits controlling vertebrate locomotion: Moving in a new direction. Nat Rev Neurosci 10: 507–518.

Goulding M, Lanuza G, Sapir T, Narayan S. 2002. The formation of sensorimotor circuits. Curr Opin Neurobiol 12: 508–515.

Goulding M, Pfaff S. 2005. Development of circuits that generate simple rhythmic behaviors in vertebrates. Curr Opin Neurobiol 15:14–20.

Grillner S, Hellgren J, Ménard A, Saitoh K, Wikström M. 2005. Mechanisms for selection of basic motor programs—Roles for the striatum and pallidum. Trends Neurosci 28:364–370.

Jaworski A, Long H, Tessier Lavigne M. 2010. Collaborative and specialized functions of Robo1 and Robo2 in spinal commissural axon guidance. J Neurosci 30:9445–9453.

Jessell TM. 2000. Neuronal specification in the spinal cord: Inductive signals and transcriptional codes. Nat Rev Genet 1:20–29.

Kewley R, Whitelaw M, Chapman Smith A. 2004. The mammalian basic helix-loop-helix/PAS family of transcriptional regulators. Int J Biochem Cell Biol 36:189–204.

Kiehn O, Kullander, K. 2004. Central pattern generators deciphered by molecular genetics. Neuron 41:317–321.

Lanuza G, Gosgnach S, Pierani A, Jessell T, Goulding M. 2004. Genetic identification of spinal interneurons that coordinate left-right locomotor activity necessary for walking movements. Neuron 42:375–386.

Lundfald L, Restrepo CE, Butt SJB, Peng C, Droho S, Endo T, Kiehn O. 2007. Phenotype of V2-derived interneurons and their relationship to the axon guidance molecule EphA4 in the developing mouse spinal cord. Eur J Neurosci 26:2989–3002.

Lyuksyutova A, Lu C, Milanesio N, King L, Guo N, Wang Y, Zou Y. 2003. Anterior-posterior guidance of commissural axons by wnt-frizzled signaling. Science 302:1984–8.

Madisen L, Zwingman TA, Sunkin SM, Oh SW, Zariwala HA, Gu H, Ng LL, et al. 2010. A robust and high-throughput Cre reporting and characterization system for the whole mouse brain. Nat Neurosci 13:133–140.

Mambetisaeva E, Andrews W, Camurri L, Annan A, Sundaresan V. 2005. Robo family of proteins exhibit differential expression in mouse spinal cord and robo-slit interaction is required for midline crossing in vertebrate spinal cord. Dev Dyn 233:41–51.

Mansouri A, Voss AK, Thomas T, Yokota Y, Gruss P. 2000. Uncx4.1 is required for the formation of the pedicles and proximal ribs and acts upstream of Pax9. Development 127:2251–2258.

Marion J, Yang C, Caqueret A, Boucher F, Michaud J. 2005. Sim1 and Sim2 are required for the correct targeting of mammillary body axons. Development 132:5527–5537.

Meijer D, Kane M, Mehta S, Liu H, Harrington E, Taylor C, Rowitch D. 2012. Separated at birth? The functional and molecular divergence of OLIG1 and OLIG2. Nat Rev Neurosci 13:819–831.

Michaud JL, Rosenquist T, May NR, Fan CM. 1998. Development of neuroendocrine lineages requires the bHLH-PAS transcription factor SIM1. Genes Dev 12: 3264–3275.

Moran-Rivard L, Kagawa T, Saueressig H, Gross MK, Burrill J, Goulding M. 2001. Evx1 is a postmitotic determinant of v0 interneuron identity in the spinal cord. Neuron 29:385–399.

Nissen U, Mochida H, Glover J. 2005. Development of projection-specific interneurons and projection neurons in the embryonic mouse and rat spinal cord. J Comp Neurol 483:30–47.

Okada A, Charron F, Morin S, Shin D, Wong K, Fabre P, McConnell S. 2006. Boc is a receptor for sonic hedgehog in the guidance of commissural axons. Nature 444:369–373.

Pearson KG. 1993. Common principles of motor control in vertebrates and invertebrates. Annu Rev Neurosci 16: 265–297.

Pierani A, Moran Rivard L, Sunshine MJ, Littman DR, Goulding M, Jessell TM. 2001. Control of interneuron fate in the developing spinal cord by the progenitor homeodomain protein Dbx1. Neuron 29:367–384.

Raper JA. 2000. Semaphorins and their receptors in vertebrates and invertebrates. Curr Opin Neurobiol 10:88–94.

Reeber S, Sakai N, Nakada Y, Dumas J, Dobrenis K, Johnson J, Kaprielian Z. 2008. Manipulating robo expression in vivo perturbs commissural axon pathfinding in the chick spinal cord. J Neurosci 28:8698–8708.

Rossignol S, Dubuc R, Gossard J. 2006. Dynamic sensorimotor interactions in locomotion. Physiol Rev 86:89–154.

Saueressig H, Burrill J, Goulding M. 1999. Engrailed-1 and netrin-1 regulate axon pathfinding by association interneurons that project to motor neurons. Development 126: 4201–4212.

Schweitzer J, Löhr H, Bonkowsky J, Hübscher K, Driever W. 2013. Sim1a and Arnt2 contribute to hypothalamospinal axon guidance by regulating Robo2 activity via a Robo3-dependent mechanism. Development 140:93–106.

Talpalar AE, Bouvier J, Borgius L, Fortin G, Pierani A, Kiehn O. 2013. Dual-mode operation of neuronal networks involved in left-right alternation. Nature 500:85–88.

Xu C, Fan C. 2007. Allocation of paraventricular and supraoptic neurons requires Sim1 function: A role for a Sim1 downstream gene PlexinC1. Mol Endocrinol 21: 1234–1245.

Yam P, Charron F. 2013. Signaling mechanisms of nonconventional axon guidance cues: The shh, BMP and wnt morphogens. Curr Opin Neurobiol 23:965–973.

Yip Y, Mehta N, Magdaleno S, Curran T, Yip J. 2009. Ectopic expression of reelin alters migration of sympathetic preganglionic neurons in the spinal cord. J Comp Neurol 515:260–268.

Zagoraiou L, Akay T, Martin J, Brownstone R, Jessell T, Miles G. 2009. A cluster of cholinergic premotor interneurons modulates mouse locomotor activity. Neuron 64: 645–662.

Zhang J, Lanuza GM, Britz O, Wang Z, Siembab V, Zhang Y, Goulding M. 2014. V1 and v2b interneurons secure the alternating flexor-extensor motor activity mice require for limbed locomotion. Neuron 82:138–150.

Zhang Y, Narayan S, Geiman E, Lanuza G, Velasquez T, Shanks B, Goulding M. 2008. V3 spinal neurons establish a robust and balanced locomotor rhythm during walking. Neuron 60:84–96.

Zou Y, Stoeckli E, Chen H, Tessier-Lavigne M. 2000. Squeezing axons out of the gray matter: A role for slit and semaphorin proteins from midline and ventral spinal cord. Cell 102:363–375.